

Dissolution of a secondary europium phase in monocrystalline sodium chloride

J. García M.,* J. Hernández A.,† E. Carrillo H., and J. Rubio O.

Instituto de Física, Universidad Nacional Autónoma de México, P.O. Box 20-364, Mexico 20, D. F., Mexico

(Received 4 December 1979)

A detailed study of the thermal resolution of a segregated phase of divalent europium in the sodium chloride lattice has been performed using optical-absorption and electron-paramagnetic-resonance techniques. The dissolution of the segregated phase consists mainly of a two-stage process; in the first stage (290–500 K) the isolated I-V dipoles and the segregated phase inclusions are present. In the second stage (500–700 K) the thermal decomposition of the segregated phase takes place. In order to determine the structure of the secondary europium phase, x-ray-diffraction and electron-microscopy analyses were performed on samples with different doping levels and subjected to various annealing treatments. In all cases, the segregated phase was found to be the stable dihalide phase EuCl_2 which crystallizes in a rhombohedral $C23$ structure. No evidence of a metastable phase, such as the so-called Suzuki phase, was found in our crystals. From the analysis of the increase in the concentration of I-V dipoles as a function of the annealing temperature, dimers were found to be the products of solution of the aggregates. It was also determined that the solubility of associated europium in NaCl is characterized by the energy of solution 0.46 ± 0.02 eV. Two different optical-absorption spectra for the Eu^{2+} ions in NaCl were observed. One of them (I) corresponds to the case in which the impurity is dispersed in the lattice forming I-V dipoles. It consists of two broad bands in the uv range peaking at 243 and 348 nm. The other one (II) is associated with the stable dihalide phase EuCl_2 in the sodium chloride lattice, and it also consists of two broad bands in the uv range but with peaking at 261 and 349 nm. For both spectra I and II, values for the half width and for the oscillator strength of each of the observed bands are reported. Measurements of the Vickers microhardness were also performed, and the results established that those crystals in which the impurity is dispersed in the lattice forming I-V dipoles are harder than those in which the stable dihalide phase EuCl_2 is present.

I. INTRODUCTION

To date numerous studies have been made of divalent-doped alkali-halide single crystals because the divalent impurity ions lead to the incorporation in a solid solution of an equal number of cation vacancies which can be studied using a great variety of techniques. The cation vacancies are created in order to preserve the overall charge neutrality of the crystal. The divalent cations and cation vacancies can be present in the lattice (i) independent of each other as free vacancies and free divalent ions, (ii) associated in pairs forming dipoles, or (iii) associated together in higher-order complexes than pairs. One of the simplest defects which is induced by the introduction of the divalent impurity in the alkali halides is the complex formed by the impurity ion and the cation vacancy, i.e., an I-V dipole. However, when the impurity concentration is greater than the solubility limit, the impurities leave the solid solution building up microprecipitates in the crystal. The aggregation of divalent impurities has been usually monitored by means of dielectric relaxation, ionic thermocurrents

(ITC), optical-absorption, electron-paramagnetic-resonance (EPR), and luminescence techniques. The occurrence of precipitates as a consequence of the aggregation has been established from x-ray-diffraction spectra, electron-microscopy measurements, light scattering, as well as by the use of the Mössbauer spectroscopy. It has been found, that in addition to the stable dihalide phase, different types of metastable phases can be formed, depending on the doping level, annealing treatment, and on the crystal system.

The first measurements dealing with the kinetics of aggregation of divalent impurities in the alkali-halide crystals were performed by Cook and Dryden¹ using dielectric absorption techniques. These authors found that during the first stage of aggregation the rate of disappearance of dipoles was proportional to the third power of the dipole concentration. This result implies that the first aggregation product is a cluster of three I-V dipoles, i.e., a trimer. The decay curve was followed by a dipole-trimer equilibrium, and by the formation of higher-order complexes. The observation of a third-order kinetics was very

surprising since a random encounter of two dipoles is much more probable than a three-body event.

Recently, Unger and Perlman² have shown, using the data taken by Cook and Dryden and some others by themselves, that the aggregation of impurity-vacancy dipoles in NaCl and KCl follows a second-order kinetics if the reverse process, i.e., dissociation, is taken into account in the dipole decay theory.

Although the isothermal decay of I-V dipoles as a function of time has been extensively studied³⁻⁷ for a large number of different divalent impurity ions in NaCl and KCl, few investigations dealing with the study of the reverse process,⁸⁻¹¹ i.e., the dissolution of an aggregated or precipitated component of the solid solution, have been reported.

In the present paper a detailed study of the thermal resolution of a secondary phase of divalent europium in monocrystalline sodium chloride is presented. In order to monitor the increase in the number of I-V dipoles, which results from the thermal decomposition of the precipitated phase, optical-absorption and electron-paramagnetic-resonance (EPR) techniques were employed. This work was undertaken (i) to determine the structure of the secondary phase of Eu^{2+} in NaCl, (ii) to identify any features of both the EPR and the optical-absorption spectrum which could be specific to the precipitated phase, (iii) to obtain the energy of solution of associated europium in sodium chloride, (iv) to determine the products of solution of the precipitated phase, and (v) to establish the influence of the Eu^{2+} ion in the Vickers microhardness of the NaCl host crystal.

II. EXPERIMENTAL

Single crystals of sodium chloride doped with divalent europium were grown at our laboratory using the Czochralski method under a controlled atmosphere (dry argon) in order to minimize contamination by OH, H_2O , and oxygen which are present in air and could affect the solubility and precipitation phenomena. Doping was achieved by adding to the melt different initial concentrations of EuCl_2 which was previously reduced from $\text{EuCl}_3 \cdot 6 \text{H}_2\text{O}$ using standard techniques.¹²

The EPR data were obtained using a conventional reflection-type spectrometer operating at X-band frequencies and a cylindrical cavity operating in the TE_{011} mode. Crystal orientation was achieved using a goniometer which allowed rotation of the crystal in a plane perpendicular to the one in which the magnet was rotated. Optical-absorption measurements were made with a Perkin Elmer Coleman EPS-3T double-beam recording spectrophotometer. The concentration of the impurity in the samples was determined directly from the optical-absorption spectrum using our previously determined calibration constants

between the optical-absorption coefficient of the high-energy band and the number of divalent europium ions expressed in ppm.¹³ Chemical analysis was also done with atomic-absorption spectrophotometry in order to determine the background impurities in the crystal selected. To do that, a Perkin Elmer model 304 spectrophotometer was employed. It was found that the background impurities were always at least two orders of magnitude below the dopant concentrations used in this work (~ 300 up to ~ 6000 ppm) for the intentional divalent europium impurity. In order to measure the Vickers microhardness an indenter of diamond in the form of a square pyramid with an apex angle of 136° and a Reichert Universal microscope "MeF" were employed.

III. RESULTS AND DISCUSSION

If one adds EuCl_2 to the NaCl powder, the doubly valent Eu^{2+} impurity ion enters the NaCl lattice substitutionally during growth of the crystal and replaces the single charged Na^+ ion. In order to preserve the overall charge neutrality of the crystal, a positive-ion vacancy which is usually located in the neighborhood of the impurity producing an effective I-V dipole is created. For the specific case of Eu^{2+} in the alkali halides, the defect formed by the impurity ion and the cation vacancy located at the position of nearest neighbors has been studied using EPR techniques by Aguilar *et al.*,^{14,15} Muñoz *et al.*,¹⁶ and Rubio *et al.*^{17,18} In all cases, it was found, that the impurity europium ion occupies a C_{2v} site symmetry in these crystals.

The Eu^{2+} ion in NaCl produces two broad optical-absorption bands in the ultraviolet which are due to transitions from the $4f^7 {}^8S_{7/2}$ ground state of the Eu^{2+} ion, to states in the $4f^6 5d$ configuration.¹⁹ The high-energy band is a transition from the ground state to the e_g component of the $4f^6 5d$ configuration, while the low-energy band is a transition from the ground state to the t_{2g} component. The separation between them is due to the well-recognized splitting $10Dq$ (Dq is the cubic field splitting of the e_g and t_{2g} orbitals) of the $5d$ orbitals by the crystal field into two distinct energy levels. Figure 1 shows the optical-absorption spectrum I for the Eu^{2+} ion in NaCl at 300 K corresponding to a recently grown crystal. To obtain this spectrum the sample was heated after growth for 20 h at 800 K, and then air quenched to room temperature. Therefore, the optical-absorption spectrum I can be associated to the case in which the impurity is dispersed in the lattice forming I-V dipoles. In the same figure we have included the optical-absorption spectrum II which was obtained from a four-year-old crystal and for which most of the impurity could be found forming a segregated phase. It is important to note that the sample

used to obtain spectrum II was stored at room temperature and was not subject to any previous heat treatment since it was grown, four years ago. By an inspection of Fig. 1, it is possible to conclude that one of the main differences between spectra I and II is the position of the high-energy band. In II this band peaks at 261 nm and has a well-resolved structure even at room temperature. In I it peaks at 243 nm and presents much less structure. Furthermore, the ratio of the intensities of the high- and low-energy bands is ~ 1 for spectrum I but it is almost ~ 2 for spectrum II. When an old crystal was quenched by dropping it into a copper block after heating for 2 h at 800 K, the band at 261 nm disappeared and the one at 243 nm was formed; i.e., spectrum II was transformed into I. The integral intensity of the optical-absorption spectrum I was found to be the same as the one previously measured in II, before the heat treatment. This fact suggests that a constant number of Eu^{2+} ions is involved and that differences in spectra I and II arise from a change of environment of the impurity ions. It was also observed that the 243-nm band faded into the 261-nm band after several weeks of aging at room temperature. The latter two facts suggest that spectrum II in NaCl arises from a Eu aggregated center. In fact, when these aged crystals from which spectrum II was observed were placed in the beam of a He-Ne laser, they displayed a large amount of light scattering which indicates that precipitation had taken place. Light-scattering measurements performed on doped samples with ~ 600 ppm of Eu^{2+} revealed that the Eu particle phase was ~ 1000 Å in diameter and was very homogeneously distributed throughout the crys-

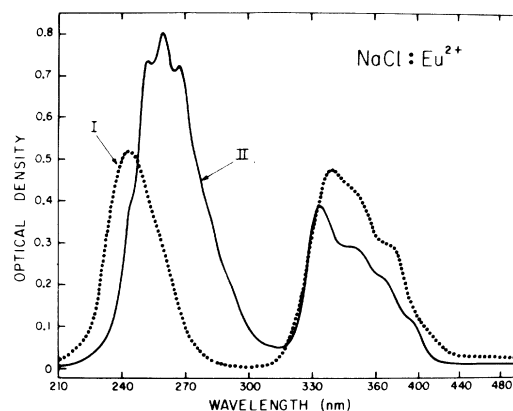


FIG. 1. Room-temperature optical-absorption spectra of Eu^{2+} in NaCl for a freshly grown crystal (I) and for a four-year-old crystal (II). (Crystal thickness: 0.6 mm.)

tal. At this point, it is important to mention that those well-aged crystals from which spectrum II was observed, exhibited in all cases, a green color. However, when the samples were heated for 2 h at 800 K and then air quenched to room temperature, the color changed to purple and spectrum I was observed. This evidence gives additional information about the state of the europium impurity in the NaCl matrix without performing any other measurements.

In Table I the peak positions, the width (W), and the values for the oscillator strength (f) are reported for each of the observed bands in the optical-absorption spectra I and II of Eu^{2+} in NaCl and for a sample temperature of 295 K. In order to calculate

TABLE I. Observed bandwidths and oscillator-strength values at 295 K.

Host	High-energy band				Low-energy band			Total oscillator strength (10^{-2})
	Peak positions (10^3 cm^{-1})	Bandwidth (10^3 cm^{-1})	Oscillator strength (10^{-2})	Total oscillator strength (10^{-2})	Peak positions (10^3 cm^{-1})	Bandwidth (10^3 cm^{-1})	Oscillator strength (10^{-2})	
NaCl (I)	41.12	6.02	3.87	3.87	25.48	2.01	0.21	2.31
					26.95	1.45	0.33	
					27.70	1.15	0.19	
					28.41	1.05	0.21	
					29.20	1.47	0.54	
					30.44	1.86	0.83	
NaCl (II)	34.67	1.42	0.29	3.94	25.35	1.04	0.12	1.63
	35.70	1.12	0.29		26.21	1.05	0.10	
	36.58	1.10	0.43		26.95	1.10	0.18	
	37.48	1.12	0.72		27.72	1.14	0.19	
	38.65	1.29	0.99		28.60	1.21	0.27	
	39.90	1.27	0.80		29.24	1.18	0.18	
41.07	1.45	0.42	30.28	1.36	0.59			

values for the oscillator strength two steps were followed: (i) a decomposition of the observed structured bands into Gaussian-shape bands was performed and their width, and intensity were varied until a good fit to the experimental-absorption spectra was obtained. Figure 2 shows, as an example, the fit for the high-energy band of the optical-absorption spectrum II. It should be noted that the width reported in Table I for each of the observed bands is the one obtained following the procedure mentioned above, and (ii) once the width and the intensity of each of the bands were known, values for f were calculated using the most appropriate form of Smakula's equation given by

$$Nf = 8.7 \times 10^{16} [n / (n^2 + 2)^2] \alpha_{\max} W,$$

where W is the width of the band at half maximum in eV, α_{\max} is the maximum absorption coefficient in cm^{-1} , n is the refractive index at the peak of the band, f is the oscillator strength, and N is the ion density in ions/ cm^3 . The concentration (N) of Eu^{2+} in the samples was directly obtained from the optical spectra using our previously determined calibration constant between N in ppm and the absorption coefficient α in cm^{-1} of the short-wavelength band. With this procedure, values for the oscillator strength were calculated to within $\pm 10\%$. The obtained values for f are very similar to those previously reported by Low²⁰ for Eu^{2+} in CaF_2 , and by Butement²¹ for $\text{EuCl}_2:\text{SrCl}_2$ and $\text{EuCl}_2:\text{BaCl}_2$ liquid solutions.

In Table II values are reported for the measured 10- Dq splitting of spectra I and II, along with those previously reported by Hernández *et al.*¹⁹ for the same ion in other alkali-halide host crystals. In the same table, the value for the 10- Dq splitting reported by Ganopolskii *et al.*²² for EuCl_2 in liquid solution is also included for the sake of comparison. This value is very similar to the one we have measured for spectrum II of Eu^{2+} in NaCl and gives some indication

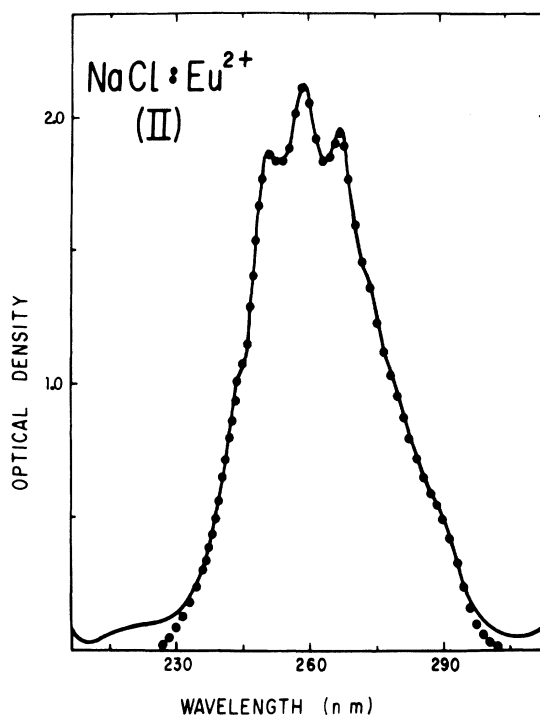


FIG. 2. High-energy absorption band at 261 nm of Eu^{2+} in NaCl (spectrum II) showing the fitting to the experimental curve using the data reported in Table I. (Crystal thickness: 1 mm.) The solid line represents the experimental curve and the points the calculated one.

that the precipitated phase of divalent europium in the sodium chloride lattice could be EuCl_2 . The preliminary conclusion obtained only from the analysis of the optical-absorption spectrum II is in agreement as it will be shown later, with the identification of the precipitated phase which was made using x-ray-diffraction techniques.

TABLE II. Values for the 10- Dq splitting of Eu^{2+} in several hosts at 295 K.

Host	Center of gravity of the high-energy band (cm^{-1})	Center of gravity of the low-energy band (cm^{-1})	10 Dq (cm^{-1})	Ref.
NaCl (I)	41 118	28 714	12 404	Hernández <i>et al.</i> and this work
NaCl (II)	38 228	28 628	9 600	This work
$\text{EuCl}_2:\text{H}_2\text{O}$	40 486	31 250	9 236	Ganopolskii <i>et al.</i>
Liquid solution				
KCl	41 102	28 852	12 250	Hernández <i>et al.</i>
RbCl	40 950	29 030	11 920	Hernández <i>et al.</i>
KBr	39 809	28 509	11 300	Hernández <i>et al.</i>
RbBr	39 216	29 061	10 155	Hernández <i>et al.</i>
KI	37 202	28 210	8 992	Hernández <i>et al.</i>

Figure 3 shows the lower-magnetic-field portion of the EPR spectrum corresponding to a four-year-old crystal before any heat treatment and for a sample temperature of 295 K. The static magnetic field is applied along the crystallographic [001] direction. The initial EPR spectrum at room temperature is weak indicating that the "associated" solubility of europium in NaCl is low. However, an increase in the solubility after heating the sample for 2 h at 800 K and then air quenched to room temperature can be observed in the lower part of Fig. 3. The optical-absorption spectrum corresponding to each situation was also included in the same figure for the sake of comparison. The origin of the fine-structure groups in the EPR spectra of Eu^{2+} in NaCl has been described by Aguilar *et al.*¹⁴ From an angular variation of the magnetic field in the (100) and (110) planes, these authors were able to identify the orthorhombic-symmetry spectra due to Eu^{2+} ions in six inequivalent sites. It was found that the z axis of the six inequivalent sites lies along the direction of equivalent $\langle 001 \rangle$ crystalline axis and their x and y axes lie along equivalent $\langle 110 \rangle$ directions. With the static magnetic field applied along the crystallographic [001] direction, we observed 14 groups in the EPR spectra. Since the electronic spin of divalent europium is $\frac{7}{2}$, there are two contributions—one labeled z

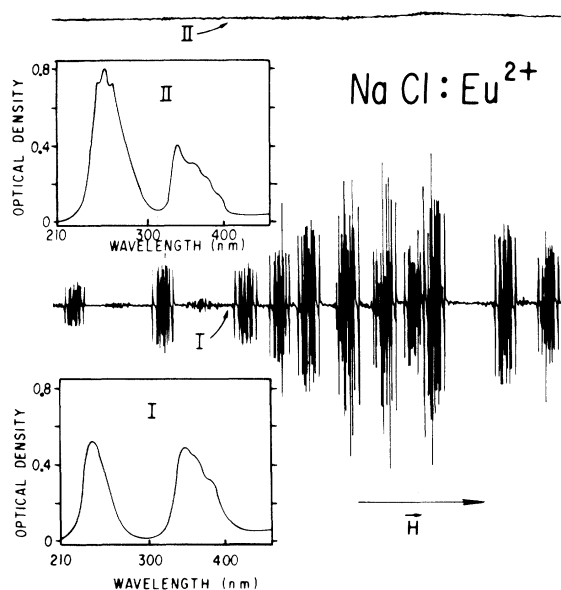


FIG. 3. Part of the EPR spectrum of Eu^{2+} in NaCl with $\vec{H} \parallel [001]$ corresponding to a four-year-old crystal (II) before any previous heat treatment, and after the same sample was heated for 2 h at 800 K and then air quenched to room temperature (I). In both cases the recording conditions of the EPR spectrometer were the same. The optical-absorption spectrum corresponding to each situation is also included for the sake of comparison.

and the other xy (following the notation of Aguilar *et al.*) to the spectrum with $\vec{H} \parallel [001]$. These spectra are produced by distortions from the normal cubic environment. Each spectrum is made up of a superposition of several spectra which are identical except that they have different sets of equivalent principal axes. The z contribution to the spectrum is due to the [001] and $[00\bar{1}]$ sites which are equivalent when the field is applied along this particular direction. The xy contribution is due to the equivalence between [010], $[0\bar{1}0]$, [100], and $[\bar{1}00]$ sites with $\vec{H} \parallel [001]$. (The sites are designated according to their z axis direction.) Measurements of the change of intensity of the fine-structure groups in the EPR spectra will reveal the changes of dipole population. It should be noted that the initial EPR spectrum of a well-aged crystal consists mainly of a broad line located at $g \sim 2$ which disappears after heating the sample. A similar broad line has been observed in the EPR spectrum of Mn^{2+} in monocrystalline sodium chloride by Watkins.²³ This author associated the broad line to aggregated manganese ions near internal boundaries or dislocations. He also reported that heating the crystal produces the disappearance of the broad line and that other spectra appeared due to the association of the Mn^{2+} ion with cation vacancies located at the position of nearest or next-nearest neighbors. From this fact he concluded that heating the sample produces the thermal destruction of the manganese aggregates and puts the impurity into solid solution.

Figures 4 and 5 show the evolution of the optical-absorption and EPR spectrum, respectively, for a four-year-old crystal as a function of the annealing time. In order to obtain these spectra, the sample

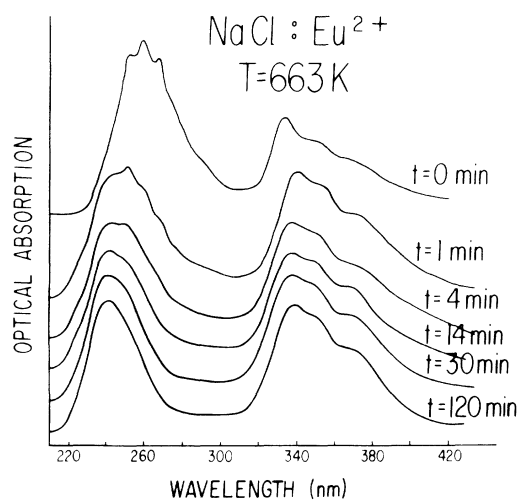


FIG. 4. Evolution of the optical-absorption spectrum (II) of Eu^{2+} in NaCl as a function of the annealing time.

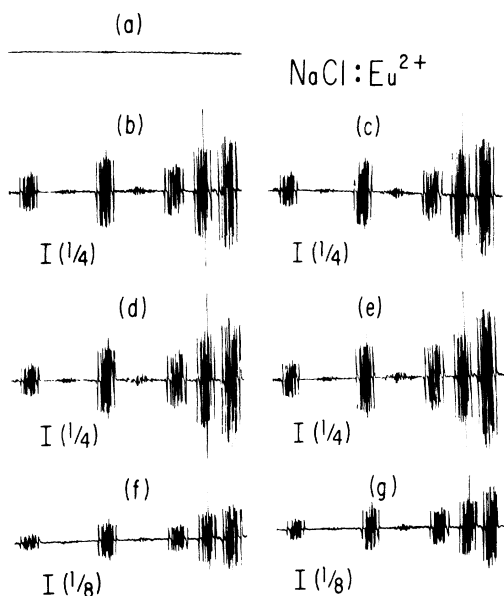


FIG. 5. Evolution of the low-field part of the EPR spectrum of Eu^{2+} in NaCl with $\vec{H} \parallel [001]$ corresponding to a four-year-old crystal as a function of the annealing time at 663 K: (a) 0, (b) 1, (c) 3, (d) 4, (e) 14, (f) 30, and (g) 120 min. Note the reduction of the signal level (I).

was heated at 663 K for the periods of time shown in the figures, and then air quenched to room temperature to record both the EPR and the optical-absorption spectra. The spectrum II was converted into I after heating the sample for 2 h at 663 K. When this conversion occurred the intensity of the EPR spectrum reached a saturated value. Heating the crystal for longer periods of time did not produce any change in the optical absorption nor in the EPR spectra. Heat treatments at higher temperatures produced the transformation of spectrum II into I in shorter periods of time. However, the temperature mentioned above was selected to make this study, since the evolution of both the EPR and the optical-absorption spectra can be followed in quite reasonable times. From Figs. 4 and 5, it is possible to observe that the dipole concentration in the sample increased with the annealing time. Figure 6 shows the quantitative results of this analysis. In order to make this plot a decomposition of the observed spectrum into I and II was made at each time, and from the resulting intensity of the high-energy band of spectrum I the concentration (N) of dipoles was determined using the calibration constant previously reported by Hernández *et al.*¹³ between the optical-absorption coefficient of this band and N in ppm. To measure the concentration of dipoles at each time using the EPR spectrum the following procedure was used: The total concentration of Eu^{2+} -cation vacancy

pairs (I-V dipoles) in the sample, which was previously determined from the optical-absorption spectrum, was associated to the saturated intensity of the fine-structure groups in the EPR spectra for the case in which the magnetic field was applied along the [001] direction. As it was mentioned before, the saturated intensity of the fine-structure groups was achieved after heating the sample for 2 h at 663 K. Then, the observed intensities of the fine-structure groups, at each time, were compared to those corresponding to the saturated values. To do this, the EPR spectra were recorded under the same conditions. Care was taken to select the fine-structure groups to be compared in the EPR spectrum since some of them appeared superimposed with $\vec{H} \parallel [001]$, and therefore, making difficult the performance of meaningful comparisons. To make this analysis the transitions $|\pm \frac{7}{2}\rangle \leftrightarrow |\pm \frac{5}{2}\rangle$, $|\pm \frac{5}{2}\rangle \leftrightarrow |\pm \frac{3}{2}\rangle$, and $|\pm \frac{3}{2}\rangle \leftrightarrow |\pm \frac{1}{2}\rangle$ of the z spectrum and the $|\pm \frac{5}{2}\rangle \leftrightarrow |\pm \frac{7}{2}\rangle$, $|\pm \frac{3}{2}\rangle \leftrightarrow |\pm \frac{5}{2}\rangle$, and $|\pm \frac{1}{2}\rangle \leftrightarrow |\pm \frac{3}{2}\rangle$ of the xy spectrum were selected. It should be noted that 11 values for the dipole concentration at each intermediate time were obtained by the use of this procedure. However, they did not differ by more than 10%. Therefore, an average value of these measurements was taken as representative of the dipole concentration at each time. The results obtained in this form are reported in Fig. 6 along with those obtained from the analysis of the optical-absorption spectrum. Good agreement was found between both analyses.

Figures 7 and 8 show the evolution of the low-field portion of the EPR spectrum and of the optical-absorption spectrum II, respectively, as a function of the annealing temperature for an Eu^{2+} -doped NaCl crystal which was grown four years ago and then stored at room temperature. The sample was not

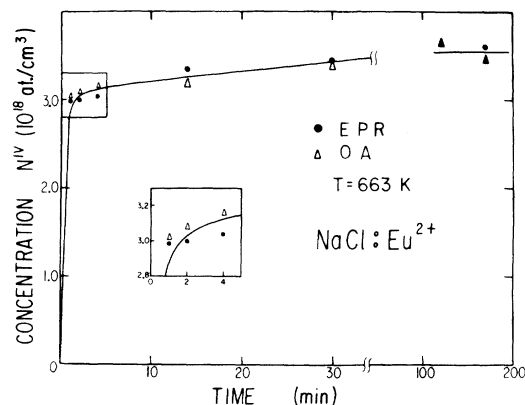


FIG. 6. Concentration of I-V dipoles as a function of the annealing time at $T = 663$ K measured with the use of: (●) electron paramagnetic resonance and (Δ) optical-absorption (OA) techniques.

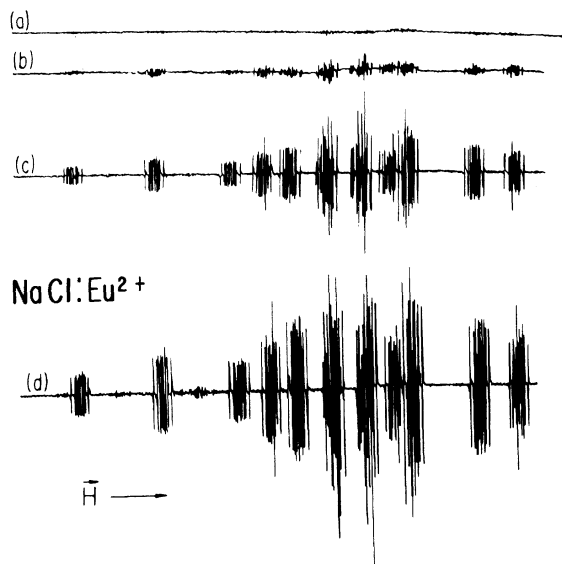


FIG. 7. Evolution of the EPR spectrum of Eu^{2+} in NaCl with $\vec{H} \parallel [001]$ as a function of the annealing temperature: (a) 300, (b) 370, (c) 422, and (d) 558 K.

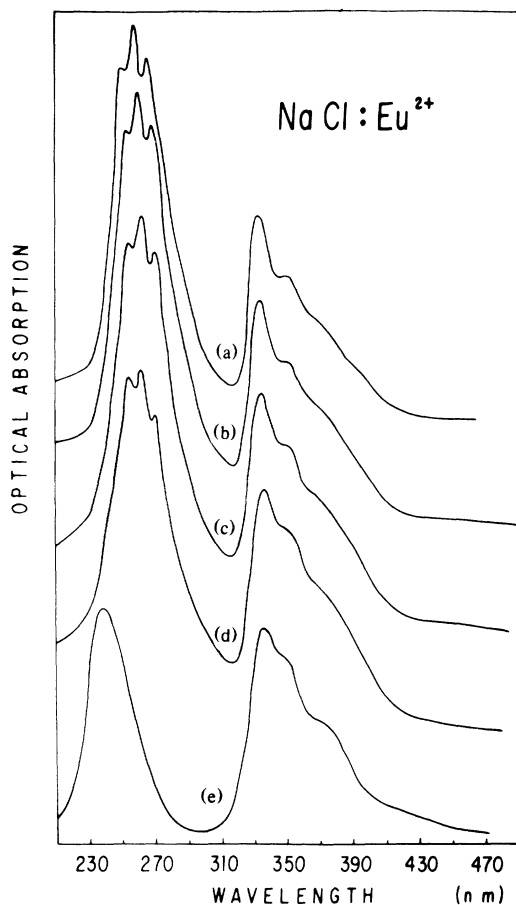


FIG. 8. Evolution of the optical-absorption spectrum (II) of Eu^{2+} : NaCl as a function of the annealing temperature: (a) 300, (b) 485, (c) 558, (d) 600, and (e) 780 K.

subject to any previous heat treatment before the measurements. To monitor the change in concentration of the dipoles caused by the thermal decomposition of the secondary phase of Eu^{2+} , EPR and optical-absorption techniques were employed. To make these measurements, the sample was heated for 30 min at the temperatures shown in the figures and then air quenched to room temperature to record both the EPR and the optical-absorption spectra. To determine the concentration of dipoles at each temperature, the same procedure as the one previously described was employed. Results are shown in Fig. 9 which establish that the thermal resolution of the aggregated impurity, which results in the dipole growth, is a three-stage process. In the first stage (290–370 K) the isolated I-V dipoles and the precipitated Eu-phase inclusions are present. At an aging temperature of ~ 370 K an increase of $\sim 10\%$ takes place in the dipole concentration which reaches a saturated value in the temperature region of 370–530 K. This is the second stage. The thermal decomposition of the segregated phase occurs in the third stage (500–700 K) which is characterized by a rapid increase in the dipole concentration. Once the temperature of 664 K was reached, the sample was heated for 2 h at this temperature. After this treatment, which puts the impurity into solid solution, precipi-

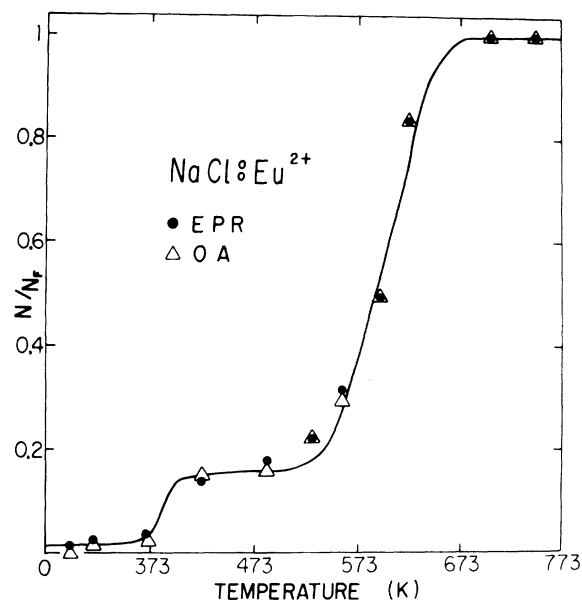


FIG. 9. Concentration of I-V dipoles vs the annealing temperature measured with the use of: (●) electron paramagnetic resonance and (Δ) optical-absorption techniques, for a four-year-old crystal of $\text{NaCl}:\text{Eu}^{2+}$ without any previous heat treatment. N_f represents the total concentration of Eu^{2+} -cation vacancy pairs (i.e., I-V dipoles) in the sample while N represents the concentration of dipoles at the intermediate annealing temperatures.

tates were induced by linear cooling from 663 K to room temperature at a rate of 15 K/h. Then, the same type of analysis as the one previously described was made and the results are shown in Fig. 10. By an inspection of Figs. 9 and 10 one can conclude that the results obtained, in both cases, are very similar. The main difference is that the second stage in the thermal resolution of the segregated phase does not appear in Fig. 10. This evidence suggests that the 10% increase in the dipole concentration at ~ 370 K for a four-year-old crystal without any previous heat treatment, may be due to the thermal decomposition of small clusters of the precipitated phase or of some simple aggregates. Figure 11 shows an Arrhenius plot of the results presented in Figs. 9 and 10. From the slope of curve D, which represents the dipole growth, an energy of solution of 0.46 ± 0.02 eV for the solubility of the associated europium ion in NaCl was obtained. This value can be compared with those previously reported for the associated solubility of the divalent impurity ions Sr^{2+} (0.49 eV),¹¹ Ca^{2+} (0.30 and 0.67 eV),^{24,25} Mg^{2+} (0.34 eV),²⁴ Ba^{2+} (0.76 eV),²⁴ Zn^{2+} (0.48 eV),²⁶ Cd^{2+} (0.40 eV),²⁴ and Mn^{2+} (0.33 and 0.7 eV) (Refs. 24 and 27) in monocrystalline sodium chloride. The slope of the monotonic decrease of curve P which corresponds to the thermal resolution of the precipitated phase was found to be twice as that of D at high temperatures. From this result one can deduce that two I-V dipoles are the products of solution of the aggregates which may be

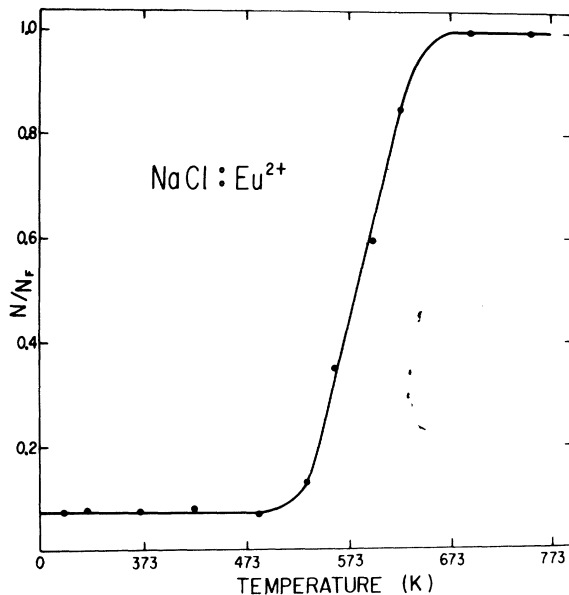


FIG. 10. Concentration of I-V dipoles vs the annealing temperature for a $\text{NaCl}:\text{Eu}^{2+}$ crystal which was first heated during 2 h at 663 K and then cooled to room temperature at a rate of 15 K/h.

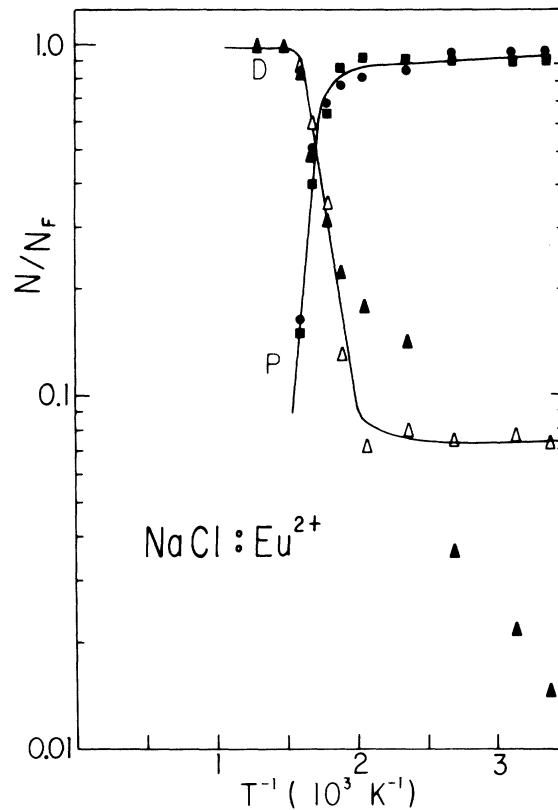


FIG. 11. Arrhenius plot of the thermal resolution of the precipitated phase (P) of Eu^{2+} in NaCl which results in the dipole growth (D). Here ● and ▲ represent the average values of the measurements reported in Fig. 9 for a four-year-old crystal, while ■ and Δ represent the measurements reported in Fig. 10 for a crystal which was first heated during 2 h at 663 K and then cooled to room temperature at a rate of 15 K/h.

dimers as suggested by the occurrence of a second-order kinetics in the first stage of precipitation of divalent impurities in NaCl and KCl according to the analysis performed by Unger and Perlman.²

Precipitation of a phase containing divalent ions from an alkali-halide solid solution can take different structural forms. In addition to the dihalide phase, different types of metastable phases are formed, depending on the crystal system, annealing treatment, and doping level. Suzuki²⁸ was able to extract precipitates of a new phase in NaCl doped with 30 mol% CdCl_2 , which were identified to have a similar structure to sodium chloride but with a double cell size and the stoichiometry $6 \text{NaCl}:\text{CdCl}_2$. This determination motivated the search for similar precipitation structures in other hosts and with other impurities. Since then, the metastable precipitated Suzuki phase has been found in the systems $\text{NaCl}:\text{MgCl}_2$,²⁹ $\text{NaCl}:\text{NiCl}_2$,³⁰ $\text{NaCl}:\text{FeCl}_2$,³¹ and $\text{NaCl}:\text{MnCl}_2$.³²

although it does not form in NaCl-CaCl₂ nor in NaCl-BaCl₂ (Ref. 33) after a whole variety of heat treatments. For these two systems the stable dihalide phases CaCl₂ and BaCl₂ have been found to be formed. For the system NaCl-SrCl₂, both the Suzuki and the stable dihalide phases have been reported to nucleate. Sors and Lilley³⁴ found in slowly cooled NaCl single crystals grown from the melt containing 1 mol% SrCl₂, that the precipitating phase of Sr²⁺ in this crystal is the stable cubic dihalide phase SrCl₂. From the analysis of x-ray-diffraction photographs the crystal lattice of the precipitates was found to be parallel to that of the NaCl matrix. Recently, however, Hartmanová *et al.*¹¹ reported that the precipitating phase of Sr²⁺ in their NaCl crystals, which were stored at room temperature for two years, was the metastable Suzuki phase. This identification was made comparing the observed ITC spectrum of Sr²⁺ in NaCl with that previously reported by Cappelletti *et al.*³⁵ for KCl-PbCl₂ and which was associated to the precipitated Suzuki phase of the lead ion in potassium chloride.

The lattice energy of the Suzuki-phase structure 6 NaCl:MCl₂ has been calculated by Sors and Lilley³⁶ as a function of the M⁺⁺ radius and anion displacements. These authors arrived at the conclusion that the nucleation of the Suzuki phase is favored in NaCl, if the ratio between the radii of the impurity ion and the host-cation ion is less than 1.2. This result has been supported by the fact that no 6 NaCl-MCl₂ phases have been detected with large M⁺⁺ radii. Since r^{++}/r^+ is for NaCl doped with Eu²⁺ roughly at the mentioned limit, it is interesting to identify the structure of the precipitating phase in this system in order to compare with the theoretical predictions mentioned above. This identification was done in our crystals using x-ray-diffraction techniques and the results showed that in NaCl:Eu²⁺, the precipitated phase is the stable dihalide phase EuCl₂. It is known³⁷ that EuCl₂ crystallizes in a simple rhombohedral system with the lattice constants $a = 7.429$ Å, $b = 8.914$ Å, and $c = 4.493$ Å in the crystallization type C23. The growth of the EuCl₂ precipitates in the sodium chloride lattice can be described in the same manner as the one reported by Vlasák and Hartmanová³⁸ for the stable dihalide phase BaCl₂. No evidence of Suzuki-phase inclusions was found in our crystals, although different doping levels (~300–~6000 ppm) and annealing treatments were employed. This determination is in agreement with that previously reported by José-Yacamán and Basset,³⁹ who found using electron microscopy, that the decoration patterns for the system NaCl-EuCl₂ were very similar to those of NaCl-CaCl₂ for which the stable dihalide phase is known to be formed. Parallel with our studies, José-Yacamán performed a new investigation trying to find Suzuki-phase inclusions in our crystals; however, although different an-

nealing treatments and doping levels were employed, all the attempts were unsuccessful. The case of the NaCl-EuCl₂ system ($r^{++}/r^+ = 1.06$) is similar to that of NaCl-CaCl₂ ($r^{++}/r^+ = 0.95$), and LiF-FeF₂ ($r^{++}/r^+ = 1.11$) in the sense that no Suzuki-phase inclusions has been observed in those systems. Despite the fact that for NaCl-EuCl₂ r^{++}/r^+ is less than 1.2 which is required for the formation of the Suzuki phase, no evidence of its existence was detected for the range of doping levels and annealing treatments employed in this work. In view of this, it appears that the size criterion is not sufficient and that more precise criteria for the nucleation of the Suzuki phase will be necessary, mainly for those cases in which r^{++}/r^+ is close to 1.2.

Finally, it is well known that both radiation damage and doping by divalent impurity ions produce a significant strengthening of the alkali halides. Sill and Martin⁴⁰ have shown that both Sr²⁺ and Eu²⁺ increase the hardness of the KCl crystal, although Eu²⁺ is significantly less effective than Sr²⁺. Since the divalent europium ion in the sodium chloride lattice occupies a similar symmetry site as in KCl, an increase in the hardness behavior should also be observed in the NaCl:Eu²⁺ crystal in comparison with the pure one.

In order to determine the influence of the Eu²⁺ ion in the hardness of NaCl, a set of measurements of the Vickers microhardness was performed on samples with different doping levels and subject to different annealing treatments. Since microhardness is usually dependent on the load, the Mayer line was first drawn through the test points in order to determine the relationship between the load (P) and the diagonal (d) of the pyramid-shaped impression. This is shown in Fig. 12 for a NaCl-doped sample with an

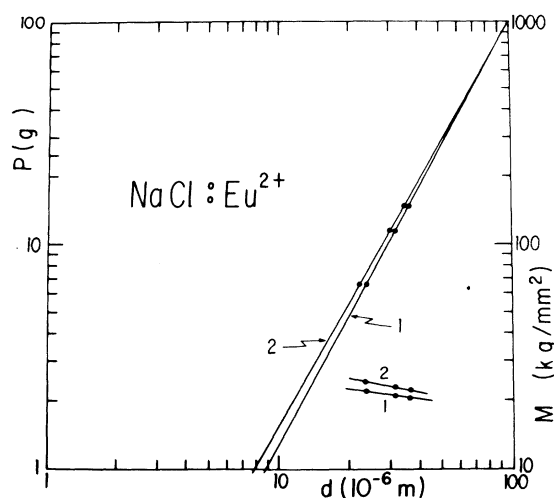


FIG. 12. Microhardness results for: (1) a well-aged NaCl crystal doped with Eu²⁺ without any previous heat treatment and (2) after the precipitated phase was destroyed. The relationship between the load (P) and the diagonal (d) of the pyramid-shaped impression of the Mayer line is also presented.

impurity concentration of 3.2×10^{18} at. Eu/cm³ using the left-hand scale. The points in this figure represent the arithmetical mean of 16 indentation diagonals for each load level. By means of number 1 we refer to the measurements performed on a four-year-old crystal before any previous heat treatment. The measurements taken on the same sample, after it was heated at 700 K for 2 h and then air quenched to room temperature, are represented by number 2. From the slope of the Mayer's lines (1) and (2), the values of 1.86 and 1.82 were obtained, respectively, for the power-law exponent (n) in the Mayer law $p = ad^n$, where a is a constant which depends on the material being tested and on the shape of the indenter, and d is the diagonal of the pyramid-shaped impression. These results mean that in both cases, the Vickers microhardness is dependent on the load. Values for the Vickers microhardness (M) of the doped sample, before and after the heat treatment, were calculated for each load using the load-dependent relationship⁴¹ (in kg/mm²)

$$M = 1854.4P/d^2,$$

where p is in grams and d in μm . The results are shown in Fig. 12 using the right-hand scale for the microhardness (M). From the results shown in this figure, one can conclude that the doped sample is harder when the impurity is dispersed in the lattice forming I-V dipoles than when the stable dihalide phase EuCl₂ is present. However, in both situations, the Vickers microhardness is larger for the doped sample than for the pure one. The same type of results as those mentioned above were obtained in heavily doped samples. The increase in the value of the Vickers microhardness of the well-aged doped samples after they were heated and the impurity was put into solid solution, can be explained as the result of the dissolution of the precipitated phase which produced a decrease in the separation between the

obstacles, and therefore an increase in the difficulty for the movement of dislocations.⁴²

Attempts were also made to correlate the hardening behavior of the NaCl-doped sample with the dissolution of the precipitating phase EuCl₂. However, the value of the Vickers microhardness did not change, within the experimental error, although the dissolution of the precipitated phase was taking place as revealed from the optical and EPR measurements. This result is in contrast with the flow-stress measurements performed on samples doped with divalent impurities which established that the hardening behavior of the sample is strongly dependent on the annealing treatment, as well as on the state of the impurity in the crystal. We believe therefore, that the Vickers microhardness technique is not very sensitive in studying the hardening behavior of the NaCl:Eu²⁺ crystal as a function of the dissolution of the precipitated phase, and that flow-stress measurements will be preferred to make this type of analysis.

ACKNOWLEDGMENTS

The authors are indebted to Dr. M. José-Yacamán for valuable suggestions and discussions throughout the course of this investigation, and for performing the electron-microscopy measurements in parallel with our studies. We also thank Professor O. Cano and Fís. A. Cordero-Borboa for taking the x-ray-diffraction data and to W. K. Cory for growing the crystals. We are greatly indebted to Dr. W. P. Unruh from Kansas University for making the light-scattering measurements. Helpful discussions with Dr. W. A. Sibley and Dr. J. J. Martin from Oklahoma State University are also gratefully acknowledged. One of us (J.G.M.) would like to thank the Proyecto de Superacion del Personal Academico for financial support.

*Facultad de Ciencias, UNAM.

†On leave from UNMSM, Lima-Perú.

¹J. S. Cook and J. S. Dryden, Proc. Phys. Soc. London **80**, 479 (1962); Aust. J. Phys. **13**, 260 (1960).

²S. Unger and M. M. Perlman, Phys. Rev. B **10**, 3692 (1974); **12**, 809, 5997 (1975); **15**, 4105 (1977).

³J. S. Dryden and G. G. Harvey, J. Phys. C **2**, 603 (1969).

⁴H. F. Symmons and R. C. Kemp, Br. J. Appl. Phys. **7**, 607 (1966).

⁵J. S. Dryden, J. Phys. Soc. Jpn. (Suppl. III) **18**, 129 (1963).

⁶J. S. Dryden, S. Morimoto, and J. S. Cook, Philos. Mag. **12**, 379 (1965).

⁷R. M. Grant and J. R. Cameron, J. Appl. Phys. **37**, 3791 (1966).

⁸R. Cappelletti and R. Fieschi, Cryst. Lattice Defects **1**, 69 (1969).

⁹R. Cappelletti and E. Okuno, J. Electrochem. Soc. **120**, 565 (1973).

¹⁰M. Hartmanová, I. Thurzo, and H. Rezabková, Cryst. Lattice Defects **5**, 117 (1974).

¹¹M. Hartmanová, I. Thurzo, and S. Besedicová, J. Phys. Chem. Solids **38**, 587 (1977).

¹²R. A. Cooley and D. M. Yost, Inorg. Synth. **2**, 71 (1946).

¹³J. Hernández A., W. K. Cory, and J. Rubio O., Jpn. J. Appl. Phys. **18**, 533 (1979).

¹⁴G. Aguilar S., E. Muñoz P., H. Murrieta S., L. A. Boatner, and R. W. Reynolds, J. Chem. Phys. **60**, 4665 (1974).

¹⁵G. Aguilar S., H. Murrieta S., J. Rubio O., and E. Muñoz P., J. Chem. Phys. **62**, 1197 (1975).

¹⁶E. Muñoz P., J. Rubio O., H. Murrieta S., G. Aguilar S., and J. L. Boldú O., J. Chem. Phys. **62**, 3416 (1975).

¹⁷J. Rubio O., E. Muñoz P., and G. Aguilar S., J. Chem.

- Phys. 61, 5273 (1974).
- ¹⁸J. Rubio O., H. Murrieta S., E. Muñoz P., J. L. Boldú O., and G. Aguilar S., *J. Chem. Phys.* 63, 4222 (1975).
- ¹⁹J. Hernández A., W. K. Cory, and J. Rubio O., *J. Chem. Phys.* 72, 198 (1980).
- ²⁰W. Low, *Nuovo Cimento* 17, 607 (1960).
- ²¹F. D. S. Butement, *Trans. Faraday Soc.* 44, 617 (1948).
- ²²V. I. Ganopolskii, V. F. Barkovskii, and N. P. Ipatova, *Zh. Prikl. Spektrosk.* 5, 805 (1966) [*J. Appl. Spectrosc. (USSR)* 9, 325 (1967)].
- ²³G. D. Watkins, *Phys. Rev.* 113, 79 (1959).
- ²⁴R. W. Dreyfus and A. S. Nowick, *Phys. Rev.* 126, 1367 (1962).
- ²⁵A. N. Murin, S. N. Banasevich, and Yu. S. Grushko, *Fiz. Tverd. Tela (Leningrad)* 3, 2427 (1961) [*Sov. Phys. Solid State* 3, 1762 (1962)].
- ²⁶S. J. Rothman, L. W. Barr, A. H. Rowe, and P. G. Selwood, *Philos. Mag.* 14, 501 (1966).
- ²⁷B. G. Lure, A. N. Murin, and R. F. Brigevich, *Fiz. Tverd. Tela (Leningrad)* 4, 1957 (1962) [*Sov. Phys. Solid State* 4, 1432 (1963)].
- ²⁸K. Suzuki, *J. Phys. Soc. Jpn.* 10, 794 (1955).
- ²⁹Y. Yal-Jammal (unpublished), quoted by A. I. Sors and E. Lilley, *Phys. Status Solidi (a)* 27, 469 (1975).
- ³⁰G. A. Andreev, M. Hartmanová, and V. A. Klimov, *Phys. Status Solidi (a)* 41, 679 (1977).
- ³¹M. J. Yacamán and R. W. Vook, in *Proceedings of the 35th Annual Electron Microscopy Society of America*, edited by G. W. Bailey (Boston, Mass. 1977), p. 258.
- ³²J. A. Chapman and E. Lilley, *J. Mater. Sci.* 10, 1154 (1975).
- ³³G. Vlasák and M. Hartmanová, *Krist. Tech.* 10, 369 (1975).
- ³⁴A. I. Sors and E. Lilley, *Phys. Status Solidi (a)* 32, 533 (1975).
- ³⁵R. Cappelletti, A. Gainotti, and L. Pareti, in *The Electrochemistry Society INC Fall Meeting, Dallas, Texas, 1975* (Electrochemical Society, Princeton, 1976), p. 277.
- ³⁶A. I. Sors and E. Lilley, *Phys. Status Solidi (a)* 27, 469 (1975).
- ³⁷*Crystal Data, Determinative Tables*, edited by J. D. H. Donnay and Helen M. Ondik (National Bureau of Standards, Gathesburg, Maryland, 1973).
- ³⁸G. Vlasak and M. Hartmanová, *Krist. Tech.* 10, 369 (1975).
- ³⁹M. José-Yacamán and G. A. Bassett, *J. Appl. Phys.* 47, 2313 (1976).
- ⁴⁰E. L. Sill and J. J. Martin, *Mater. Res. Bull.* 12, 127 (1977).
- ⁴¹*Operating Instruction and Basic Principles*, edited by C. Reichert (Optische Werke A. G., Wien, 1970), p. 8.
- ⁴²J. C. Anderson, K. D. Leaver, J. M. Alexander, and R. D. Rawlings, *Materials Science* (Nelson, New York, 1974), p. 237.